Cell Systems, Volume *15*

Supplemental information

Classification and functional characterization of regulators of intracellular STING trafficking identified by genome-wide optical pooled screening

Matteo Gentili, Rebecca J. Carlson, Bingxu Liu, Quentin Hellier, Jocelyn Andrews, Yue Qin, Paul C. Blainey, and Nir Hacohen

Supplementary Figures

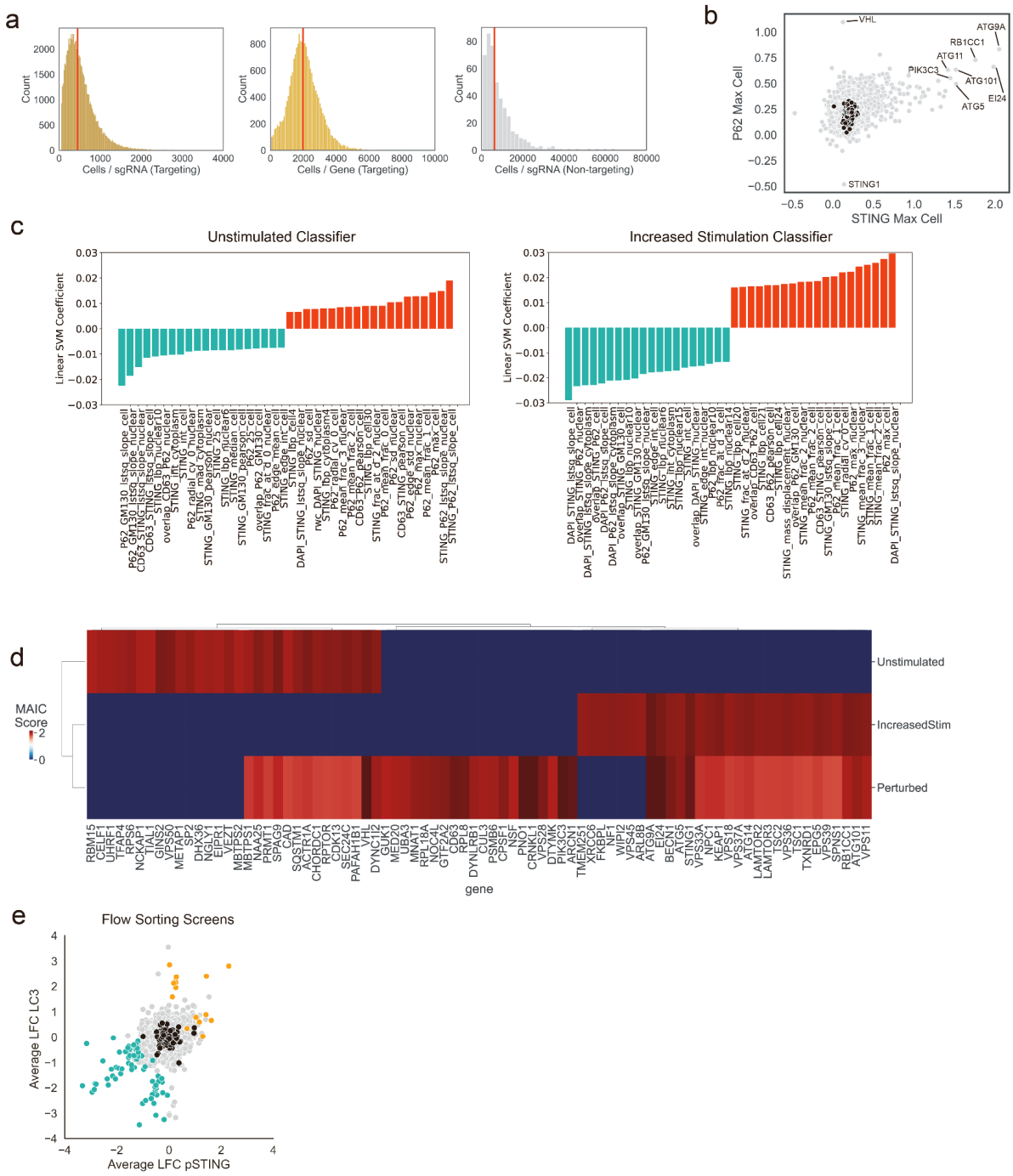

Figure S1. Genome-wide OPS, flow screens, and MAIC analysis to identify regulators of STING trafficking. Related to Fig. 1. (A) Distribution of number of cells in the screen for each sgRNA or gene for targeting sgRNAs and non-targeting controls. Medians highlighted in red. **(B)** Scatterplot of STING per-cell maximum intensity and p62 maximum intensity for each gene in the screen. Black dots indicate non-targeting control sgRNAs. **(C)** Top and bottom 20 feature weights for SVM unstimulated and increased stimulation classifiers. **(D)** MAIC scores for top 30 genes (by overall MAIC score) for each OPS

SVM classifier. **(E)** Correlation of log2 fold change (LFC) for pSTING and LC3 in STING flow cytometry screens. Orange: genes that increased both LC3 and pSTING at $p < .001$ in both screens; blue: genes that decreased both metrics at the same significance.

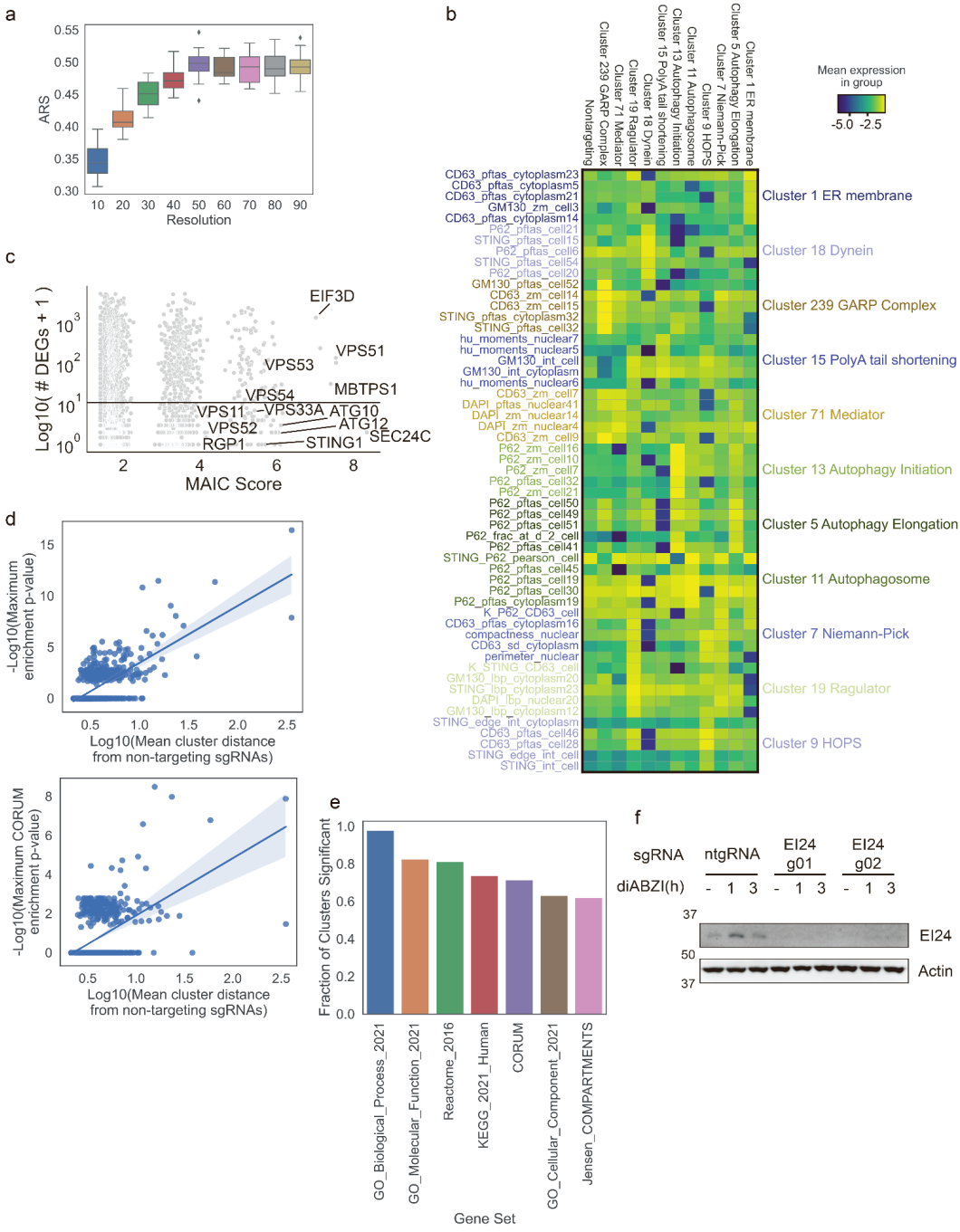
a
ARS
Resolution
b
Mean expression in group
-5.0 -2.5
Nontargeting
Cluster 239 GARP Complex
Cluster 71 Mediator
Cluster 19 Ragulator
Cluster 18 Dynein
Cluster 15 PolyA tail shortening
Cluster 13 Autophagy Initiation
Cluster 11 Autophagosome
Cluster 9 HOPS
Cluster 7 Niemann-Pick
Cluster 5 Autophagy Elongation
Cluster 1 ER membrane
Cluster 1 ER membrane
Cluster 18 Dynein
Cluster 239 GARP Complex
Cluster 15 PolyA tail shortening
Cluster 71 Mediator
Cluster 13 Autophagy Initiation
Cluster 5 Autophagy Elongation
Cluster 11 Autophagosome
Cluster 7 Niemann-Pick
Cluster 19 Ragulator
Cluster 9 HOPS
c
Log10(# DEGs + 1)
MAIC Score
EIF3D
VPS51
VPS53
MBTPS1
VPS54
VPS11
VPS33A
ATG10
ATG12
VPS52
RGP1
STING1
SEC24C
d
-Log10(Maximum enrichment p-value)
Log10(Mean cluster distance from non-targeting sgRNAs)
-Log10(Maximum CORUM enrichment p-value)
Log10(Mean cluster distance from non-targeting sgRNAs)
e
Fraction of Clusters Significant
GO_Biological_Process_2021
GO_Molecular_Function_2021
Reactome_2016
KEGG_2021_Human
CORUM
GO_Cellular_Component_2021
Jensen_COMPARTMENTS
Gene Set
f
sgRNA
ntgRNA
EI24 g01
EI24 g02
diABZI(h)
- 1 3 - 1 3 - 1 3
37
50
37
EI24
Actin

Figure S2. Clustering resolution selection and pathway enrichment analysis to identify gene clusters of interest. Related to Fig. 2. (A) Adjusted Rand score for Leiden clustering at different resolutions. **(B)** Top 5 features significantly differentiating clusters highlighted in Figure 2. **(C)** MAIC Score plotted against number of DEGs for genes included in the genome-scale Perturb-seq K562 dataset. **(D)** Scatterplots of mean cluster distance from non-targeting sgRNAs (PHATE potential distance) against the maximum enrichment p-value from Enrichr (GO, Reactome, KEGG, Jensen COMPARTMENTS and CORUM datasets, top) or from CORUM alone (bottom) **(E)** Fraction of clusters (among clusters with >1 gene and >20% of genes not non-targeting sgRNAs) that had at least one significant term as calculated by Enrichr for the noted categories. **(F)** Immunoblot of the indicated proteins in BJ1 fibroblasts transduced with a control guide (ntgRNA) or with EI24 sgRNAs and stimulated with 1μM diABZI for the indicated times.

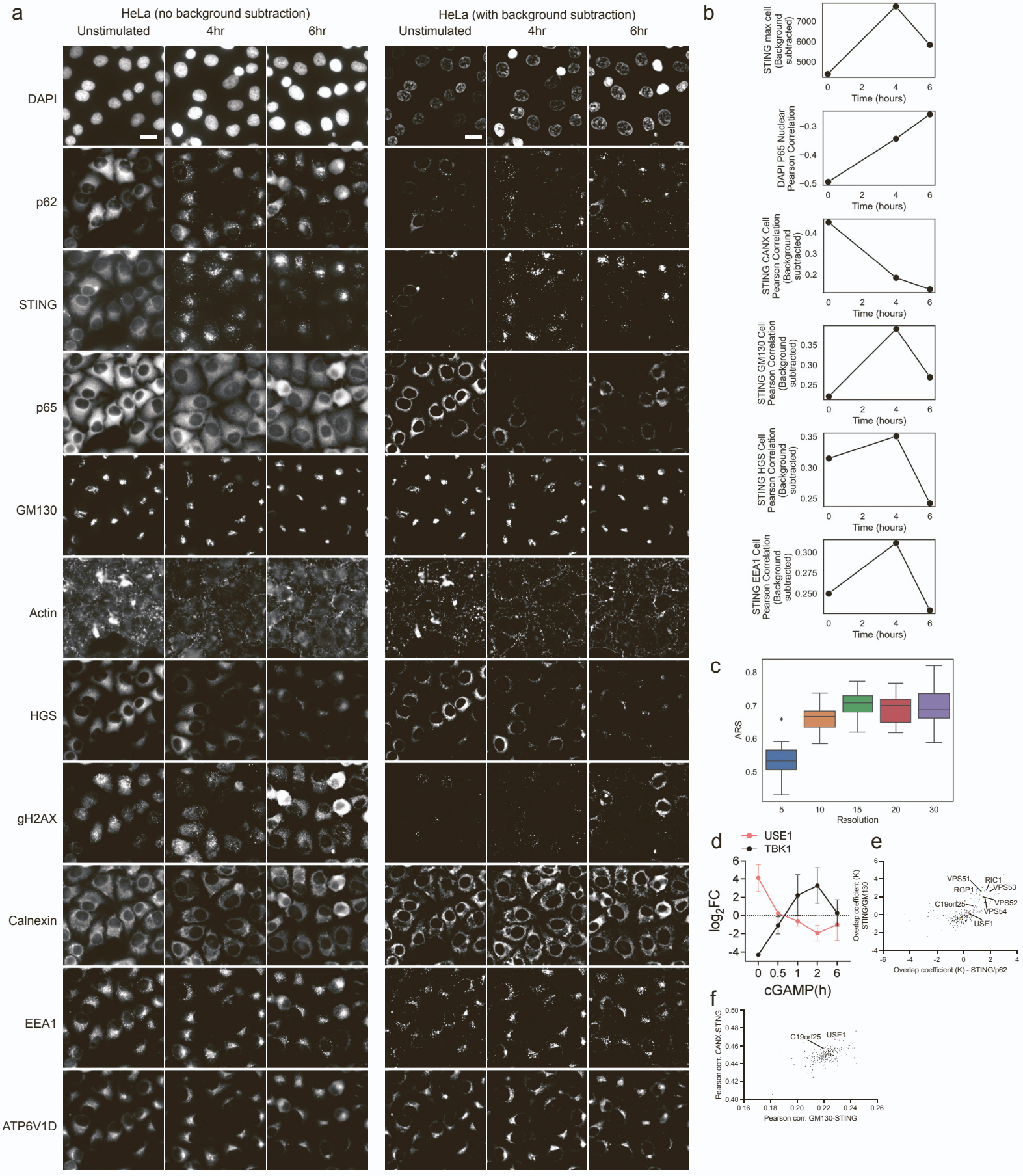
a
HeLa (no background subtraction)
Unstimulated
4hr
6hr
HeLa (with background subtraction)
Unstimulated
4hr
6hr
DAPI
p62
STING
p65
GM130
Actin
HGS
gH2AX
Calnexin
EEA1
ATP6V1D
b
STING max cell (Background subtracted)
DAPI P65 Nuclear Pearson Correlation
STING CANX Cell Pearson Correlation (Background subtracted)
STING GM130 Cell Pearson Correlation (Background subtracted)
STING HGS Cell Pearson Correlation (Background subtracted)
STING EEA1 Cell Pearson Correlation (Background subtracted)
Time (hours)
c
ARS
Resolution
d
USE1
TBK1
log2FC
cGAMP(h)
e
Overlap coefficient (K) STING/GM130
Overlap coefficient (K) - STING/p62
VPS51
RIC1
RGP1
VPS53
C19orf25
VPS52
VPS54
USE1
f
Pearson corr. CANX-STING
Pearson corr. GM130-STING
C19orf25
USE1

Figure S3. Secondary screens to identify gene clusters regulating STING trafficking. Related to Fig. 3. (A) Selected fields of view from secondary screens for HeLa cells, all channels shown. Scale bar 20 μm. **(B)** HeLa secondary screen non-targeting mean feature values across time. **(C)** Adjusted Rand score (ARS) for Leiden clustering at different resolutions. **(D)** log2 fold change (log2FC) enrichment of the indicated proteins in the STING-TurboID datasets at the indicated timepoints post cGAMP stimulation. **(E)** Overlap coefficient for the indicated channels in integrated deviation from ntgRNA from secondary OPS. **(F)** Pearson correlation of the indicated channels in unstimulated cells from the secondary OPS. **(G)** Correlation between MAIC score and number (#) of pathogenic or likely pathogenic in the Clinvar dataset. Genes of interest that we followed up upon in this (HOPS complex subunits VPS11 and VPS33A, GARP complex subunits VPS51, VPS53 related to VPS52) or previous studies (VPS37A)[8] are highlighted in red.

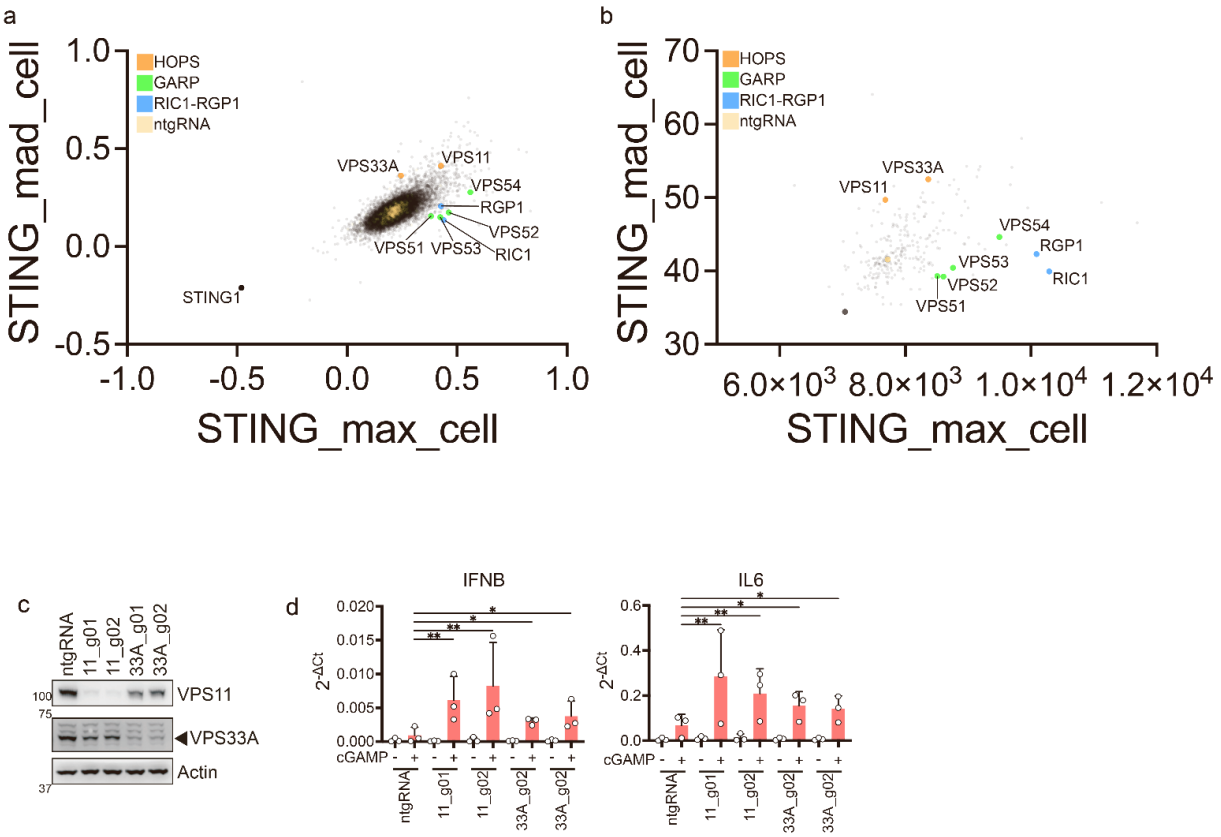

Figure S4. Identification of VPS11 and VPS33A as regulators of STING trafficking. Related to Fig. 4. (A) STING_max and STING_mad extracted features correlation in the genome-wide OPS in HeLa cells. Specific subunits of complexes of interest are indicated in color. STING1 is highlighted in black. Non-targeting control sgRNAs are indicated in yellow. Pixel intensity is normalized to ntgRNAs from unstimulated cells. **(B)** STING_max and STING_mad extracted features correlation in the secondary OPS in HeLa cells. Specific subunits of complexes of interest are indicated in color. STING1 is highlighted in black. Non-targeting control sgRNAs are indicated in yellow. Background subtracted pixel intensity values are plotted. **(C)** Immunoblot of the indicated proteins in 293T STING-mNG transduced with control (ntgRNA) or VPS11 or VPS33A sgRNAs. One blot representative of n=3 blots. **(D)** Raw $2^{-\Delta Ct}$ values related to Fig. 4e.

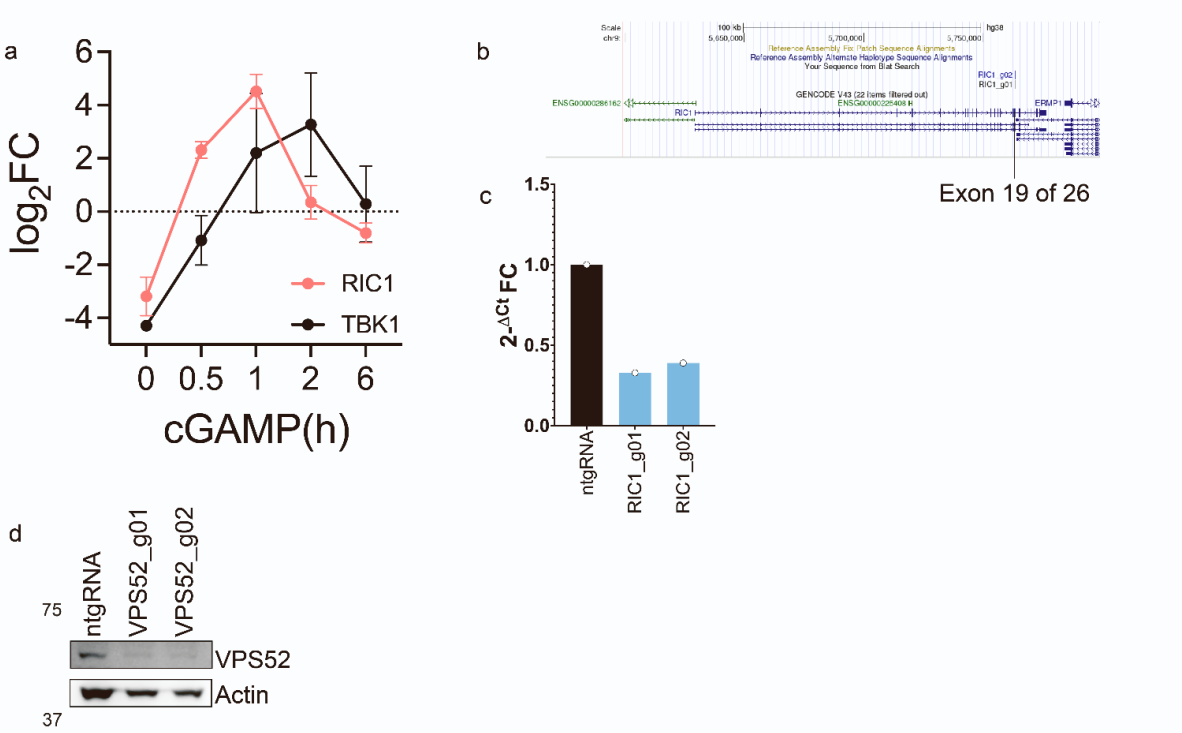

Figure S5. Identification of RIC1 and VPS52 as regulators of STING trafficking. Related to Fig. 5. **(A)** log2 fold change (log2FC) enrichment of the indicated proteins in the STING-TurboID datasets at the indicated timepoints post cGAMP stimulation. **(B)** Location of the two RIC1 targeting sgRNAs used in this paper visualized in UCSC Genome browser. While we could not identify a reliable antibody for RIC1, both guides targeted the gene in exon 19 of 26 at >50-55nt from the exon-exon junction potentially triggering Non-Sense Mediated Decay. **(C)** qPCR of RIC1 expression in 293T STING-mNG transduced with a control (ntgRNA) or RIC1 targeting guides as in b). **(D)** Immunoblot of the indicated proteins in 293T STING-mNG transduced with a control (ntgRNA) or VPS52 targeting sgRNAs.